

# Design of a Chaotic Trajectory Generator Algorithm for Mobile Robots

J. J. Cetina-Denis, R. M. López-Gutiérrez, R. Ramírez-Ramírez, C. Cruz-Hernández

**Abstract**—This work addresses the problem of designing an algorithm capable of generating chaotic trajectories for mobile robots. Particularly, the chaotic behavior is induced in the linear and angular velocities of a Khepera III differential mobile robot by infusing them with the states of the Hénon chaotic map. A possible application, using the properties of chaotic systems, is patrolling a work area. In this work, numerical and experimental results are reported and analyzed. In addition, two quantitative numerical tests are applied in order to measure how chaotic the generated trajectories really are.

**Keywords**—Chaos, chaotic trajectories, differential mobile robot, Henons map, Khepera III robot, patrolling applications.

## I. INTRODUCTION

**S**TUDIES on food searching behavior of animal groups (especially ants), helps in the solution of many problems, primarily optimization ones. Recently, biologist has discovered that ant activity is mostly of chaotic nature [1].

Research has been made on chaotic trajectory design for mobile robots in order to imitate this behavior. Some uses chaotic systems alongside the behavioral equations of differential robots to obtain a mathematical model that causes erratic motion [2]; while others [3] uses the standard map (well known discrete two-dimensional chaotic system) to generate a series of chaotic waypoints to be followed by the robot. There has been other researches [4] using a Chaotic Random Bit Generator. Also, some others [5] study the generation of chaotic behavior in mobile robots while they follow a specified path.

Among the applications given to robots with chaotic trajectories are: border patrol, dangerous object search (for example, explosives), rescue, unknown territories exploration, and others.

In this work, Hénon map is applied to give velocity values to a differential mobile robot (Khepera III in this case), to generate a chaotic trajectory that allows the robot to patrol a work area in an effective and unpredictable manner to outside spectators (like intruders).

## II. CHAOTIC SYSTEMS

Chaos theory can be defined as the qualitative study of aperiodic dynamical behavior shown by non-linear

J. J. Cetina-Denis, R. M. López-Gutiérrez and R. Ramírez-Ramírez are with the Department of Electrical Engineering, Universidad Autónoma de Baja California, Ensenada, BC, 22860 México (e-mail: jcetina@uabc.edu.mx, roslopez@uabc.edu.mx).

C. Cruz-Hernández is in the Department of Applied Physics, Centro de Investigación Científica y de Educación Superior de Ensenada, Ensenada, BC, 22860 México (e-mail: ccruz@cicese.mx).

deterministic systems. It can be observed in many natural engineering systems.

Among the principal features of chaotic systems, we find:

- High sensibility to initial conditions.
- Deterministic with an apparently random behavior.
- Oscillating, but not periodical.

Initial conditions sensibility indicates highly different temporal evolutions on the chaotic system, despite very small differences in their initial conditions. This feature is desirable on patrolling robot, since it would cause the trajectory followed by the robot to be highly unpredictable. They are deterministic because, knowing the initial conditions and the equations of the system, they behavior can be determined. With this features, we can say that a robot with a chaotic trajectory will be highly unpredictable for outside spectators, but known to the designer and any other observant that has the knowledge of the equations and the initial conditions used in its design.

### A. Hénon Map

Hénon map is a two-dimensional discrete-time dynamical system, represented by the following equations [6]:

$$\begin{aligned}x_h(n+1) &= 1 - ax_h^2(n) + y_h(n+1), \\y_h(n+1) &= bx_h(n).\end{aligned}\quad (1)$$

This map depends on a and b parameters, which classical values for chaos generation are  $a = 1.4$  and  $b = 0.3$ . For other a and b values, this map can be intermittent, converge to a periodic orbit or a fixed point. Fig. 1 shows the chaotic attractor generated by Hénon map.

### B. Fractals

The Oxford dictionary defines fractals as: A curve or geometrical figure, each part of which has the same statistical character as the whole. They are useful in modelling structures (such as snowflakes) in which similar patterns recur at progressively smaller scales, and in describing partly random or chaotic phenomena such as crystal growth and galaxy formation. The so called fractal objects are very complex and detailed. If we amplify one section of such object we find such complexity and detail as the whole object, so smaller sections are similar to the largest ones [7].

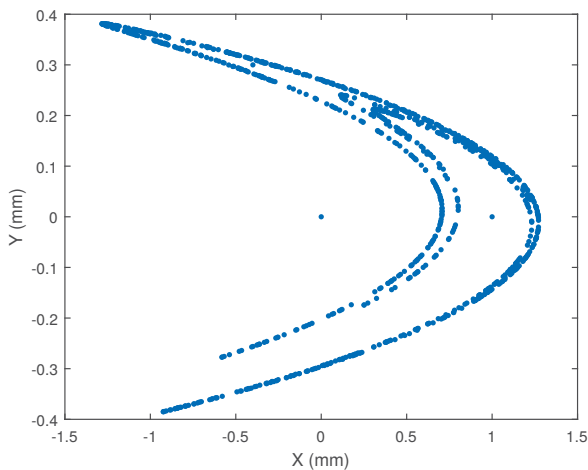


Fig. 1 Hénon map chaotic attractor

1) *Fractal Dimension*: A definition of fractal dimension is that of similarity, also called self-similarity, suggested by Felix Hausdorff in 1919, later readjusted by Besicovich (dimension of Hausdorff-Besicovich) [8]:

If  $N$  equal entities can be obtained from another entity  $H$ , similar to the original, with a similarity reason  $L$ , then the topological dimension of  $H$  is the real number  $D$  which verifies:

$$N + l^D = 1 \quad (2)$$

Meaning

$$D = \frac{\log(N)}{\log(\frac{1}{l})} \quad (3)$$

There are certain geometric objects which the  $D$  dimension is not an integer. We will call such geometric objects, using Benoit Mandelbrot terminology, *fractals*.

### III. MATHEMATICAL MODEL OF A DIFFERENTIAL MOBILE ROBOT

The behavior of a differential drive mobile robot is based on two independent wheels, one on each side of the robot's body (Fig. 2). Movement is achieved by applying different velocity values to each wheel. This way, the robot can move forward by making both wheels spin at the same speed, or it can turn in any direction using different speed for each wheel. In this work, the approximated mathematical model of the Khepera III robot will be used.

Suster-Jadlosvska [9] presents the following mathematical model for a differential drive mobile robot, observing the following considerations:

- The robot moves in a perfectly flat surface without sliding, despising wheel resistance.
- Robot position is given by  $x$ ,  $y$  and  $\theta$  coordinates, where  $\theta$  represents the robot rotation in relation to the coordinate system.

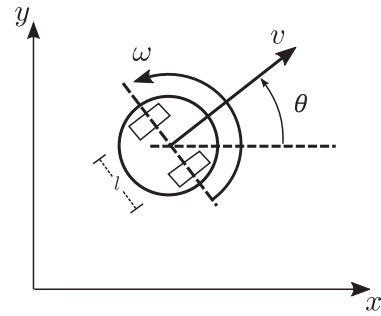


Fig. 2 Differential drive mobile robot

Position and rotation of the robot in the plane are based in the following equations, forming the kinematic model of the robot [9]:

$$\begin{aligned} \dot{x} &= v \cos(\theta), \\ \dot{y} &= v \sin(\theta), \\ \dot{\theta} &= \omega, \end{aligned} \quad (4)$$

with  $v$  and  $\omega$  defined as:

$$\begin{aligned} v &= \frac{v_l + v_r}{2}, \\ \omega &= \frac{v_r - v_l}{l}, \end{aligned} \quad (5)$$

where:  $v$ : Lineal speed,  $\omega$ : Angular speed,  $\theta$ : Robots orientation angle,  $l$ : Distance between wheels,  $l = 8.841$  cm.

### IV. METHODOLOGY

The goal of this work is the application of Hénon chaotic map (1) to generate chaotic behavior in the linear ( $v$ ) and angular ( $w$ ) speed of the differential drive robot, described by (4). To make this possible, an algorithm was designed as described in the next section.

#### A. Chaos Generator Algorithm for the Robot

The following algorithm (Fig. 3) is used for numerical simulations, experimental process and generation of chaotic trajectories in the differential robot, which is described as:

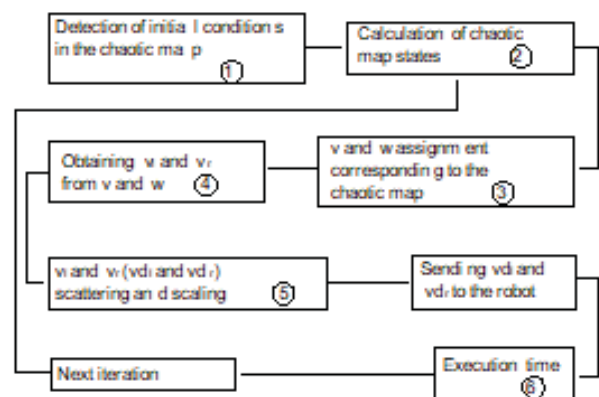


Fig. 3 Block diagram of the algorithm

The equations corresponding to every stage shown in the block diagram of Fig. 3 are as follows:

- 1)  $x_0$ : Initial position  $x$  of the robot,  
 $y_0$ : Initial position  $y$  of the robot,  
 $x_h(0) = x(0)/1000$ ,  
 $y_h(0) = y(0)/1000$ ,  
 $n = 0$ .
- 2)  $x_h(n+1) = 1 - ax_h^2(n) + y_h(n)$ ,  
 $y_h(n+1) = bx_h(n)$ .
- 3)  $v(n) = x_h(n+1)$ ,  
 $\omega(n) = y_h(n+1)$ .
- 4)  $v_l = v(n) - (l\omega(n))$ ,  
 $v_r = v(n) + (l\omega(n))$ .
- 5)  $v_{dl} = \text{floor}(((100v_l) - \text{floor}(100v_l))180) + 20$ ,  
 $v_{dr} = \text{floor}(((100v_r) - \text{floor}(100v_r))180) + 20$ .
- 6)  $t = 2$  seconds.

Isolating left and right wheel speeds from (5), we get the histograms shown in Fig. 4. We can observe that  $v_l$  values are mostly negative and  $v_r$  values are positive, indicating that the resulting trajectory will be primarily based on left turns. Because of this, dispersion and uniformity measures needs to be taken for  $v_l$  and  $v_r$  values, as shown in Fig. 5. This way, the dispersion allows to perform a re-escalation of the values to a range usable by the robot, limiting its minimum and maximum so they remain usable by the robot.

This speed range does not include negative values, preventing the robot from moving in reverse, so that the generated trajectory encompasses a larger area of coverage in a shorter time.

The two-second run time in step 6 is used to allow the robot to have the opportunity to move properly and to have greater coverage of the work area.

A HP laptop with an A10 processor of 1.9 GHz, 12 GB of RAM and Windows 10 64 bit was used. Numerical simulations and experimental work were programmed using Matlab R2015a. Flex 13 cameras were used with Optitrack's Motive™ software for verification of experimental results. The mobile robot is a Khepera III.

### B. Work Area Boundaries

The patrol area is a table measuring 1400 x 2400 mm that has edges 35 mm high. The control objective is that the differential robot covers the largest possible area of this table in a chaotic way. The robot must change its trajectory when it reaches some of the boundaries of the work area to avoid colliding with them. In this case, a reflexive movement is adopted. When the robot senses proximity to one of these limits, the robot changes its direction of movement following the strategy shown in Fig. 6. It takes an exit path at an angle that reflects the entry one.

## V. NUMERICAL RESULTS

In this part, the results obtained from the numerical simulations are reported. Starting the trajectory of the robot at the origin  $(x, y, \theta) = (0, 0, 0)$ , numerical simulations are carried out based on the chaotic generation algorithm with 200 and 300 iterations. The results obtained can be seen in

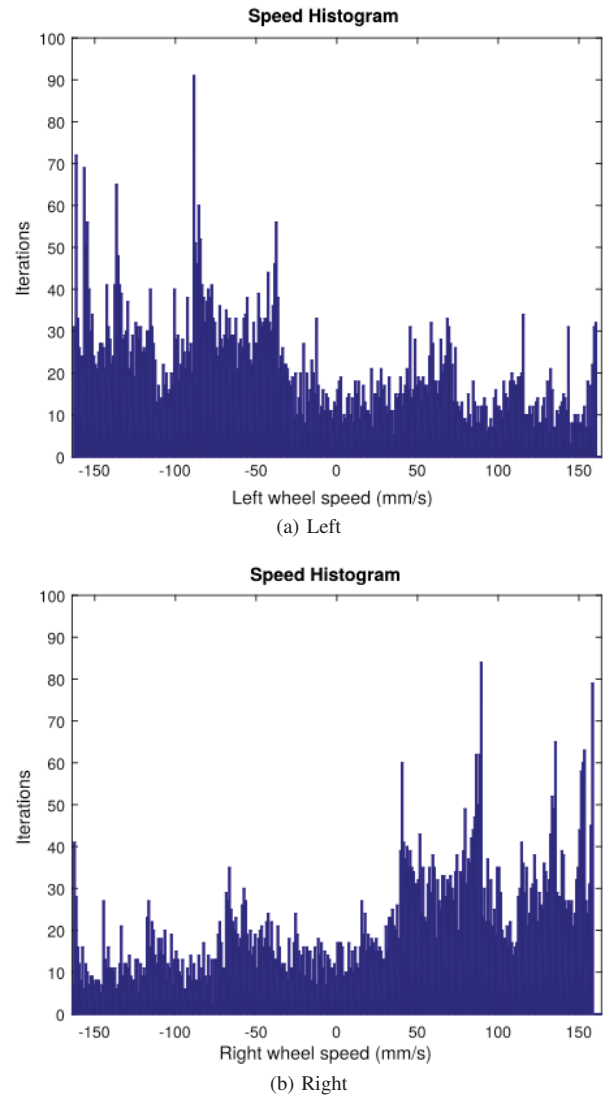


Fig. 4 Wheel speed histograms  $v_l$  and  $v_r$ .

Fig. 7. The black box represents the boundaries of the work area (table) described previously. Each color represents a time lapse of two seconds during which the robot uses the speeds obtained for each iteration before moving on to the next ones.

Fig. 7 shows that the trajectories of the robot are unpredictable and, with 300 iterations, covers (patrols) most of the work area. It is important to mention that, in the numerical simulations, the real dimensions of the robot are not considered, so the area actually covered by it is much larger than the one shown in the graphs. It can also be observed from these results (Fig. 7), that the trajectory followed in all cases under the same initial conditions is the same, confirming the deterministic nature of the chaos. On the other hand, simulations are carried out using three different initial positions (in millimeters) with the same orientation ( $\theta_0 = 0$ ) in the cases: a)  $(x_0, y_0) = (0, 0.01)$  and b)  $(x_0, y_0) = (-350, 500)$ .

For each case, 200 iterations of the algorithm are performed to compare the trajectories generated. The results are show in

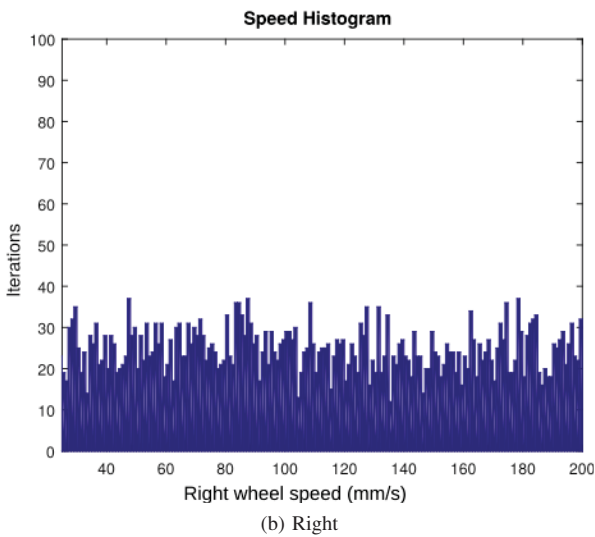
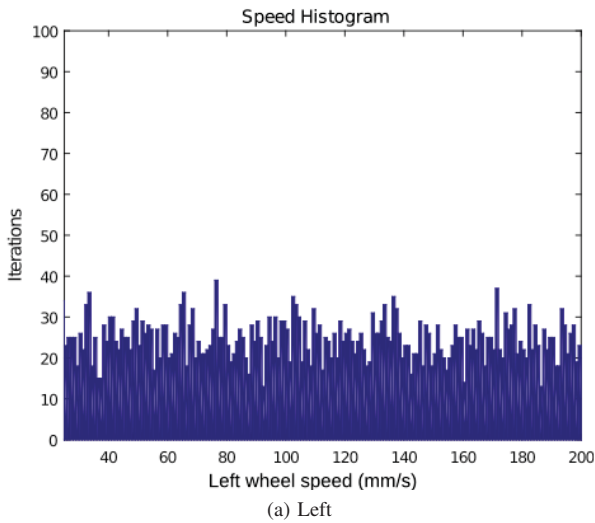


Fig. 5 Wheel speed histograms after dispersion  $v_{dl}$  and  $v_{dr}$ .

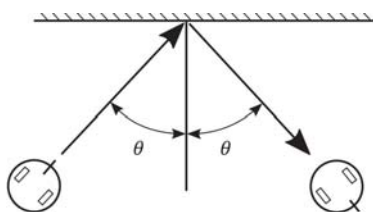


Fig. 6 Reflective edge avoidance strategy

Fig. 8.

Comparing Figs. 7 (a) and 8 (a), it can be observed that trajectories change drastically despite of having a change of only 0.01 millimeters in the  $x$ -axis, demonstrating sensitivity to initial conditions typical of a chaotic system.

1) *Coverage Percent of the Test Area:* In order to estimate the work area covered by the chaotic trajectories imposed on the mobile robot, it was divided into a grid of 12x20 (240) frames with lateral measurements of 76.66 mm, this to have a more precise idea of the effective Coverage of the algorithm proposed for exploration or search applications.

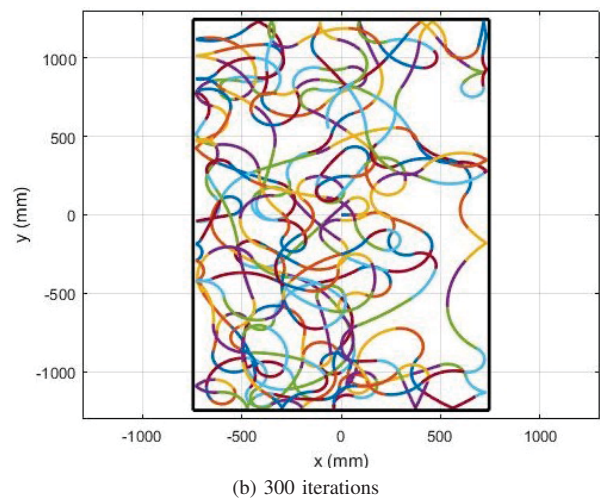
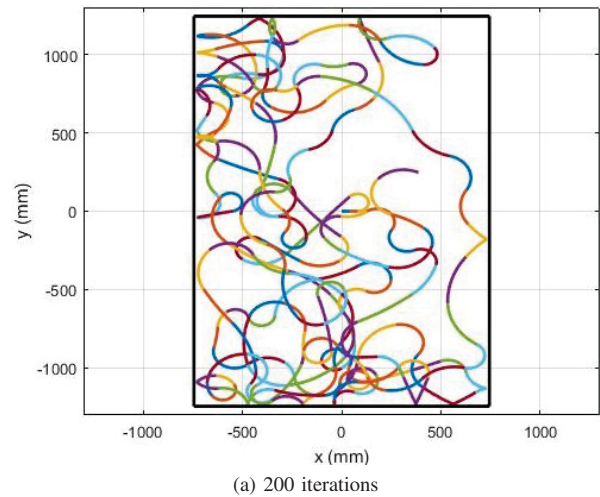


Fig. 7 Mobile robots trajectories with initial conditions  $(x_0, y_0) = (0, 0)$  with: a) 200 and b) 300 iterations

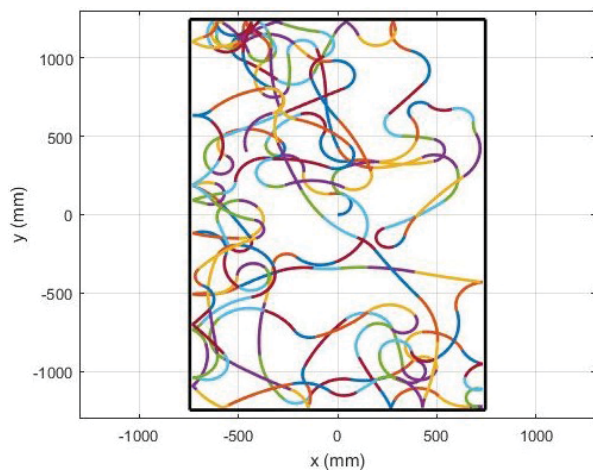
Fig. 9 shows the percentage coverage of the test area by the mobile differential robot for 100 and 300 iterations of the algorithm, when the initial conditions are  $(x_0, y_0, \theta_0) = (0, 0, 0)$ . We can see that with just 100 iterations the robot patrolled almost half of the test area and with 300 iterations covered almost the entire work surface.

Repeating the previous process 1000 times for arbitrarily selected initial conditions, an average of **84.1270%** of covered area is obtained.

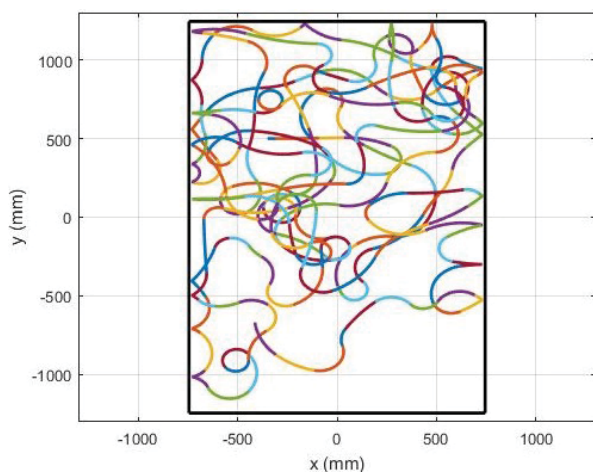
2) *Gottwald - Melbourne Test:* To verify that the trajectories generated by the algorithm proposed in this work for the robot are indeed chaotic, we use the 0-1 Gottwald-Melbourne test [10]. They describe a test to determine if a discrete deterministic dynamic system is chaotic or not. Contrary to the usual method of calculating the maximum Lyapunov exponent, this method is applied directly to the time series and does not require space-phase reconstruction. In addition, the dimension of the dynamic system and the form of its equations are irrelevant

To perform the test, 1000 iterations of the chaotic trajectory generator algorithm are executed to the mobile robot with



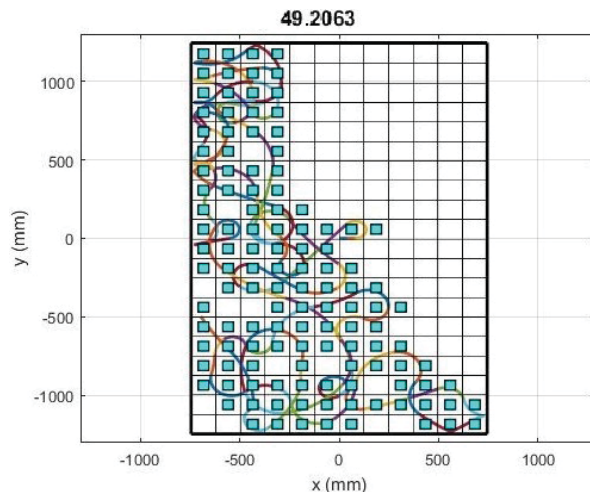


(a)  $x_0 = 0.01, y_0 = 0$

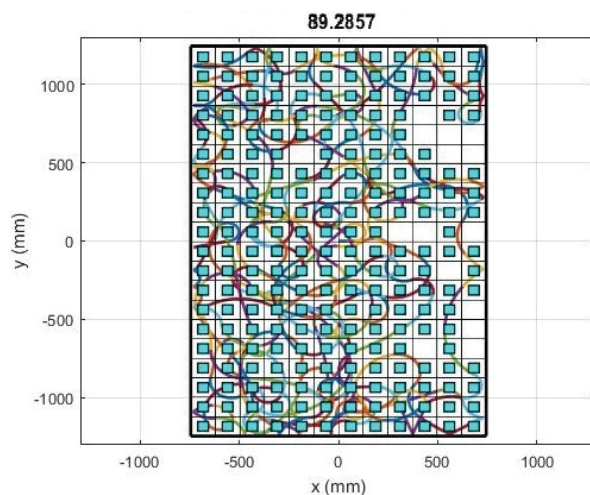


(b)  $x_0 = -350, y_0 = 500$

Fig. 8 Mobile robots trajectories by different initial conditions with 200 iterations



(a) 100 iterations



(b) 300 iterations

Fig. 9 Mobile robots trajectories with initial conditions  $(x_0, y_0, \theta_0) = (0, 0, 0)$  with: a) 100 and b) 300 iterations

different initial conditions. Taking into consideration the data of the time series of the states  $x$  and  $y$  of the model of the differential robot, obtained from the results of the numerical simulations performed, we can perform the 0-1 test to verify evidence of chaos in the trajectories of the mobile robot generated by the algorithm.

The input is the data of the time series and the output is in the range between 0 and 1, depending on whether the dynamic is chaotic or not, being 0 not chaotic and 1 totally chaotic. The test is applied to any dynamic deterministic system, see details of the test in [10].

Fig. 10 shows the time series of the  $x$  and  $y$  coordinates for the initial experimental conditions  $(x_0, y_0, \theta_0) = (0, 0, 0)$ .

The resulting value of the test for  $x$  is **0.9954** and for  $y$  is **0.9845**. The number close to 1 is a clear indication that the test concludes that such time series are indeed chaotic.

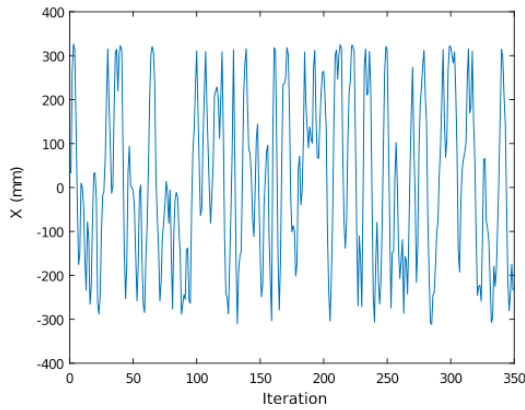
3) *Box-Counting test:* Some techniques used to estimate the fractional dimension of a geometric object were discussed by Mandelbrot [11]. In this work, the box-counting method was used because it is simple, automatically calculable with the use of computer and applicable for patterns with or without

self-similarity. In this test, each image or geometric object is covered by a sequence of squares of descendant measurements and for each of the squares two values are stored: the number of boxes intersected by the image  $N(l)$  and the lateral length of each frame  $l$ . The regression slope  $D$  of the straight line formed by the plot of  $\log(N(l))$  against  $\log(\frac{1}{l})$  indicates the degree of complexity (or fractional dimension) between 1 and 2;  $1 \leq D \leq 2$  [11]. An image with a fractional dimension of 1 or 2 is considered completely differentiable. The linear regression used to estimate the fractional dimension [12] is given by:

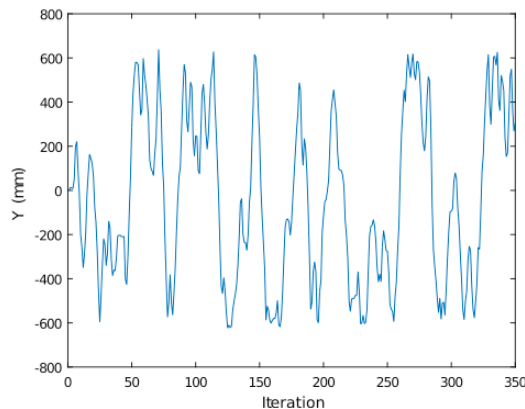
$$\log(N(l)) = \log(K) + D \log\left(\frac{1}{l}\right) \quad (6)$$

where  $K$  is a constant and  $N(s)$  is proportional to  $\frac{1}{l}^{-D}$  []. Clearing  $D$  from (6) we get the following expression,

$$D = \frac{\log(N(l))}{\log \frac{1}{l}} \quad (7)$$

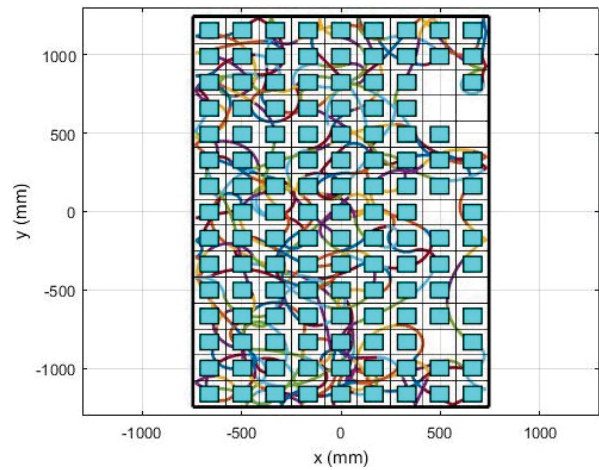


(a)  $x$  time series

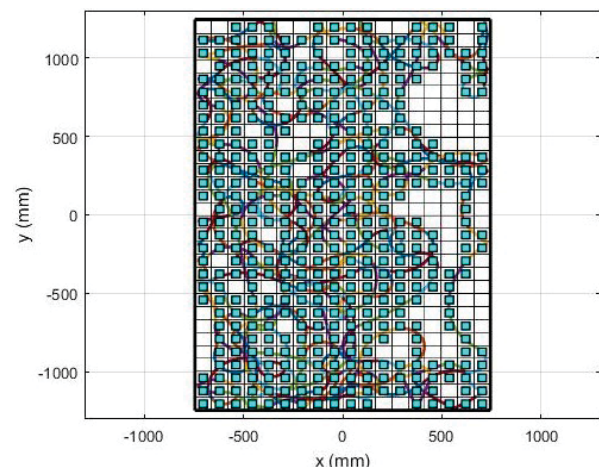


(b)  $y$  time series

Fig. 10  $x$  and  $y$  time series for initial conditions  $(x_0, y_0, \theta_0) = (0, 0, 0)$



(a) 135 boxes of  $l = 0.0625$



(b) 735 boxes of  $l = 0.0323$

Fig. 11 Different grid sizes for the Box-counting test

To perform this test, we return to the grid used to measure the percentage of coverage of the test area performed by the trajectories of the mobile robot generated by the algorithm designed in this work. The size of the grid with  $l = 1$ , will be taken for the case when the length of the work area (remember that the dimensions of the test area are  $1400 \times 2400$  mm) is equal to the length of a grid square. We start with squares of size  $l = 0.111$ , which will be reduced until obtaining very small squares (boxes) of size  $l = 0.0200$ .

We take the path of the robot generated with the initial conditions  $(x_0, y_0, \theta_0) = (0, 0, 0)$  for this test. Fig. 11 shows 2 different grid sizes for the proposed work area: a) 135 boxes of  $l = 0.0667$  and b) 735 boxes of  $l = 0.0286$ .

After making 25 reductions of the grid and plotting  $\log(N(s))$  against  $\log(\frac{1}{l})$ , the linear regression of the data results in Fig. 12. You can see a behavior very similar to the line given by the equation  $y = 1.7762x + 0.0028$ .

## VI. EXPERIMENTAL RESULTS

Two experiments with the Khepera III differential robot were performed using different initial conditions with 200 iterations for each of the following cases: a)  $(x_0, y_0, \theta_0) = (1.1, -0.9, 1.8)$  and b)  $(x_0, y_0, \theta_0) = (-0.5, -1.3, 359.1)$ .

The black square represents the boundaries of the work area (table) described above. Each color represents a time span of two seconds during which the robot uses the speed

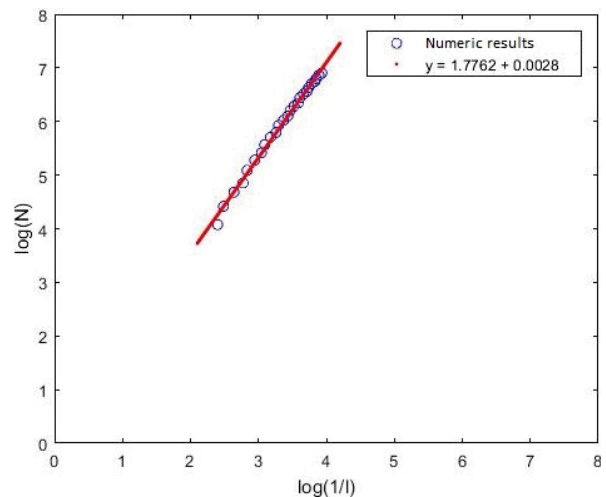


Fig. 12 Box-counting test results for initial conditions  $x_0 = 0, y_0 = 0$

values obtained by each iteration before moving to the next ones. These graphics were obtained in real time thanks to the software Motive™ and Flex 13 cameras.

The results are shown in Fig. 13.

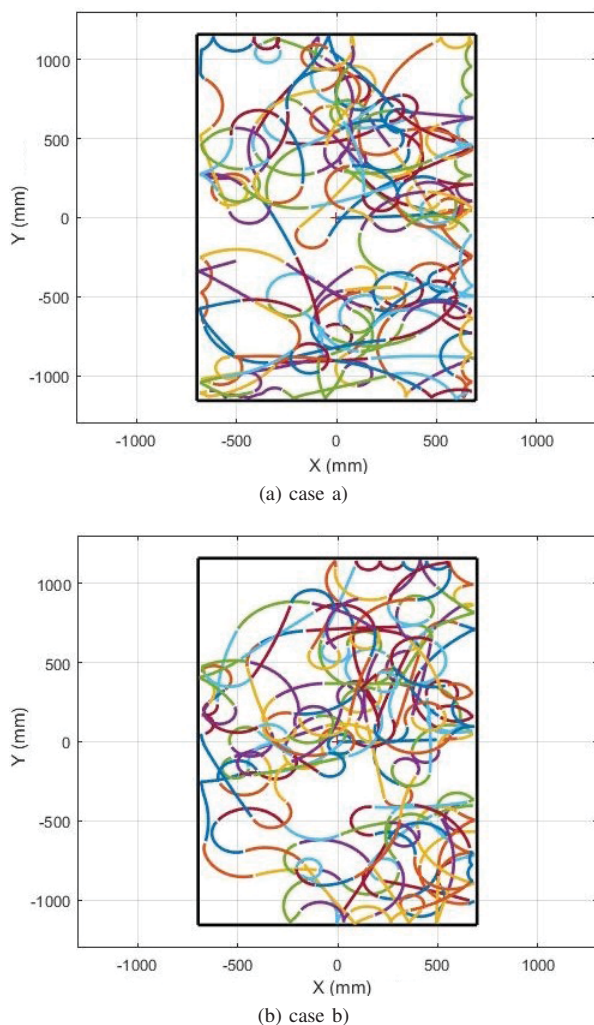


Fig. 13 Experimental results with two different initial conditions

Applying the same tests as before to this result we get a coverage percent of **91.6667** for the first case and **87.0833** for the second one. The Gottwald - Melbourne test gets **0.9546** and **0.9798** for the  $x$ -axis and **0.9136** and **0.9215** for the  $y$ -axis respectively. the Box-Counting test shows fractal dimensions for both cases as  $D = 1.7548$  and  $D = 1.7748$  respectively. These results are very similar to the ones obtained in the numerical results, and the indicate the presence of chaos in them

## VII. CONCLUSIONS

In this work the Hénon map was used to induce chaotic behavior in the linear and angular velocities of a Khepera III type mobile differential robot, with patrolling purposes taking advantage of the properties of chaos. The numerical and experimental results obtained confirm that these trajectories are unpredictable. Numerical tests were performed to determine the existence of chaos in the trajectories generated in the Khepera III mobile robot. The Gottwald-Melbourne test concludes that the time series obtained are indeed chaotic; while the box-counting test shows that the final trajectory is also chaotic.

For future work, the improvement of the edge evasion strategy is proposed, so that the experimental stage reflects with more precision the desired behavior. In addition, other chaotic systems will be implemented to compare the behavior and trajectories generated by the robot. We will work on the verification of the presence of chaos in the generated trajectories of the differential mobile robot, using other indicators of chaos.

## ACKNOWLEDGMENT

This work was funded by CONACYT, Mexico. Through the research project between institutions, Ref. 166654.

## REFERENCES

- [1] L. Li, H. Peng, J. Kurths, Y. Yang and H. Schellnhuber, *Chaos-order transition in foraging behavior of ants*. Proceedings of the National Academy of Sciences of the United States of North America, 11(23), p. 83928397, 2014.
- [2] Y. Nakamura and A. Sekiguchi, *The Chaotic Mobile Robot*. IEEE Transactions on Robotics and Automation, p. 898904, 2001.
- [3] L. Martins-Filho and E. Macau, *Kinematic control of mobile robots*. ABCM Symposium Series in Mechatronics, Volumen 2, p. 258264, 2006.
- [4] Volos, Kyprianidis and Stouboulos. *A chaotic path planning generator for autonomous mobile robots*. Robotics and Autonomous Systems, 60(4), p. 651656, 2012.
- [5] D. Curiaç and C. Volosencu *A 2D chaotic path planning for mobile robots accomplishing boundary surveillance missions in adversarial conditions*. Communications in Nonlinear Science and Numerical Simulation, 19(10), p. 36173627, 2014.
- [6] M. Hnon, *A Two-Dimensional Mapping with a Strange Attractor*. Comm. Math. Phys., 50(1), pp. 69-77, 1976.
- [7] N. Torres, *Caos en sistemas biológicos*. Matematicalia: Revista Digital de Divulgación Matemática de la Real Sociedad Matemática Española, 1(3), 2005.
- [8] A. Besicovitch, *On linear sets of points of fractional dimension*, Mathematische Annalen, 101(1): p.161193, 1929.
- [9] P. Suster and A. Jadlovska, *A Neural tracking trajectory of the mobile robot Khepera II internal model control structure*. International Conference Process, Czech Republic, Kouty nad Desnou, 2010
- [10] G. A. Gottwald and I. Melbourne, *A new test for chaos in deterministic systems*. Proceedings of the Royal Society of London A. Mathematical, Physical and Engineering Sciences. The Royal Society, Vol. 460, pp. 603611, 2004.
- [11] B. B. Mandelbrot, *The fractal geometry of nature*, Vol. 173. Macmillan, 1983
- [12] K. Foroutan-Pour, P. Dutilleul, and D. Smith, *Advances in the implementation of the box-counting method of fractal dimension estimation*. Applied Mathematics and Computation, 105(2): 195210. 1999.



**J. J. Cetina-Denis** is working towards his Ph.D. degree in Science and Engineering in Universidad Autónoma de Baja California and received the M.Sc degree in Electronics and Telecommunications in 2017 from Centro de Investigación Científica y de Educación Superior de Ensenada, BC. (CICESE), México. He has a degree in Mechatronics Engineering from Universidad Autónoma de Yucatan. His research interests are Chaotic Systems, Synchronization, Collective Behaviors, Electronics, Mechatronics, Robotics and Computer Vision.



**R. M. López-Gutiérrez** was born on 10-11-1972. She is a Professor of Electronics Engineering in Baja California Autonomous University since 2001. She received her Master Science degree and Ph.D. degree in Electronics and Telecommunications from CICESE, Mexico in 1996 and 2003, respectively. Her research interests involve synchronization of complex systems and applications.

**C. Cruz-Hernández** received the M.S. and Ph.D. degrees in electrical engineering from CINVESTAV, México, in 1991 and 1995, respectively. Since 1995, he is with the Department of Electronics and Telecommunications of the Scientific Research and Advanced Studies of Ensenada (CICESE), where, he is current Professor of Automatic Control. His research interests include multimode oscillations of coupled oscillators, nonlinear systems analysis, robotics, and synchronization and control of complex dynamical systems.

**R. Ramírez-Ramírez** is a Ph.D. student of complex systems academic group at Universidad Autónoma de Baja California (UABC), Baja California, México. He received his Master of Engineer in Technology, and Licentiate of Engineer in Technology, in electrical engineering from UABC in 2016 and 1995, respectively. In 2013 he received a certificate in embedded computer engineer from UC San Diego Extension, San Diego, CA. His master dissertation dealt with the implementation of the standard IEEE1451 within an embedded development platform. Since 1996, he has worked at Samsung, Augen and Fender as Development Engineer. In 2013-2014 he was professor of power electronics, numerical methods, embedded systems, and mechanisms at UABC.